

Polyhexamethylene Biguanide로 기능화된 하이퍼브랜치 고분자의 항균 작용 향상

Xu Meng^{****, #}, Bin Wang^{***, #}, Liping Liang^{**, †}, and Bailing Liu^{***, †}

^{*}College of Textile and Garment, Shaoxing University

^{**}College of Life Science, Shaoxing University

^{***}Chengdu Institute of Organic Chemistry, Chinese Academy of Sciences

(2016년 8월 19일 접수, 2016년 10월 4일 수정, 2016년 10월 13일 채택)

Polyhexamethylene Biguanide Functionalized Hyperbranched Polymers Enhance Their Antimicrobial Activities

Xu Meng^{****, #}, Bin Wang^{***, #}, Liping Liang^{**, †}, and Bailing Liu^{***, †}

^{*}College of Textile and Garment, Shaoxing University, Shaoxing, 312000, China

^{**}College of Life Science, Shaoxing University, Shaoxing, 312000, China

^{***}Chengdu Institute of Organic Chemistry, Chinese Academy of Sciences, Chengdu, 610041, China

(Received August 19, 2016; Revised October 4, 2016; Accepted October 13, 2016)

Abstract: Hyperbranched antibacterials show much more potential performances than their small molecules due to unique structure. Polyhexamethylene biguanide (PHMB) functionalized hyperbranched poly(amide-PHMB)s (DPBs) were prepared and their antibacterial properties were investigated using several techniques. The results showed that Gram-positive organisms were more susceptible than Gram-negative bacteria for DPBs, N¹, N³, N⁵-tris(2-aminoethyl)benzene-1,3,5-tricarboxamide (DT) and PHMB. DPBs had better comprehensive properties than DT and PHMB, and the best one was DPB1. SEM and AFM were utilized to investigate the interactions between DPB1 and bacterial membranes of *E. coli*. The mode of action of DPB1 was revealed by the morphological images, which was consistent with bactericidal mechanism of cationic antibacterial agents.

Keywords: hyperbranched polymer, polyhexamethylene biguanide, antimicrobial activity, antimicrobial mechanism.

Introduction

Dendrimers are novel highly-branched three-dimensional macromolecules that emanate from a central core and provide a very high number of end groups in the periphery.¹⁻⁶ Since dendrimers can be easily modified with lots of functional groups and possess tunable inner cavities, highly branched and surface moieties, the properties of dendrimers are very different from traditional linear analogues, such as low viscosity, ease of solubility, high reactivity, and high local concentration. Architecturally similar to dendrimers, hyperbranched polymers are a type of dendritic macromolecules, which constitute a novel class of highly branched polymers with a multitude of

end groups.⁷ Hyperbranched polymers can be prepared using a one-pot synthesis, so that they are better positioned for industrial applications.

It is well known that bacterial cell surfaces are negatively charged and often stabilized by the divalent cations, such as Mg²⁺ and Ca²⁺ presented in external environment.⁸ Hence, adsorption onto the negatively charged cell's surface is expected to be enhanced with increasing charge density of the cationic biocides. As mentioned above, hyperbranched polymer can offer a higher local density of functional groups compared with that for model compounds (monomers and polymers) and it is easily modified.⁹ If polyhexamethylene biguanide (PHMB) can functionalize hyperbranched polymer with biologically active end groups, they might be expected to show the increased antibacterial properties associated with the high local concentration.¹⁰ Meanwhile, because the binding affinity to the cytoplasmic membrane is the strongest for dendrimer and hyperbranched biocides, followed by conventional

[#]These authors contributed equally to this work.

[†]To whom correspondence should be addressed.

E-mail: blliuchem@hotmail.com; liangliping0702@163.com
©2017 The Polymer Society of Korea. All rights reserved.

polymer biocides, then by small-molecule biocides,⁹ hyperbranched biocides can be more potential than both polymeric biocides and small-molecule biocides. Therefore, hyperbranched compounds have made available new opportunities for creating more potential antimicrobial agents for both industrial and biomedical applications.

In order to increase the species of effective antimicrobial products and enhance the antibacterial activities, we designed and synthesized hyperbranched compounds. In this work, PHMB was selected as the A2 type monomer on account of its biodegradability and safety.^{11,12} This was a very important requirement, especially when these polymers were intended for use as antimicrobial drugs. Furthermore, N¹,N³,N⁵-tris(2-aminoethyl)benzene-1,3,5-tricarboxamide (DT) was selected as the A3 type branched center core to increase antibacterial effect, because its structure contain active biocidal groups (benzene acyl group). PHMB has been considered as a broad-spectrum antimicrobial material. Due to its high-water solubility, non toxicity and excellent antibacterial activity, PHMB has been widely used for many years, as an antiseptic in medicine,¹³⁻¹⁶ textiles, water treatment; as a treatment against fungi¹⁷⁻¹⁹ and disinfection of a variety of solid surfaces such as contact lenses;²⁰ as a mouthwash.^{21,22} PHMB is a mixture of polymeric biguanide with different molecular weight and various combinations of amino (-NH₂), guanide [-NH-C(=NH)-NH₂] or cyanoguanide [-NH-C(=NH)-NH-CN] as end groups.²³ Because of those active groups the biguanidine polymer can react with other compounds.²⁴⁻²⁶ So, it can be an excellent strategy for synthesizing many more biguanidine derivatives.

Antibacterial hyperbranched poly(amide-PHMB)s (DPBs) were prepared via A2+B3 reaction with different molar ratios using one-pot synthesis. The reaction molar ratios of DT and PHMB were 1:1, 1:2 and 1:3, respectively. The molecular structures of obtained hyperbranched products (DPBs) were characterized by Fourier transform infrared (FTIR) and ¹H nuclear magnetic resonance (NMR) spectra. With loading different molar ratios of PHMB into DT core, the antimicrobial properties were evaluated by the minimum inhibitory concentration (MIC), inhibition zone, UV-vis. Moreover, the antimicrobial mechanism was revealed by visualizing the bacteria morphology with scanning electron microscope (SEM) and atomic force microscope (AFM) images.

Experimental

Materials. Ethylenediamine and 1,6-hexamethylenediamine

(A.R.) were obtained from Chengdu Kelong Chemical Reagents Co., Ltd. (Chengdu, China). Concentrated sulfuric acid, sodium chloride, trimesic acid, dicyandiamide (A.R.) and Agar (gel strength > 1300 g/cm², Biosharp, Japan) were purchased from Sinopharm Chemical Reagent Co. Ltd. (Shanghai, China). Beef extract and peptone were obtained from Beijing Aoboxing Biotech Co., Ltd (Beijing, China). All reagents were used as received without further purification.

Escherichia coli (*E.coli* ATCC25922) and *Staphylococcus aureus* (*S. aureus* ATCC209P) were kindly provided by the Institute of Sichuan Antibiotic Industry, State Pharmaceutical Administration of China.

Synthesis of Hyperbranched Polymers. 1,3,5-tri(methoxycarbonyl)benzene (1): A solution of trimesic acid (21 g), methyl alcohol (250 mL) and concentrated sulfuric acid (5 mL) was refluxed for 2 h. Two-thirds of the methyl alcohol was removed by distillation. After cooling, precipitation was removed by filtration and dissolved in 300 mL of ether. The filtrate was poured into water and then extracted with ether. The ether solutions were combined, washed thoroughly with water and dried by anhydrous sodium sulfate. The ether was removed and the solid ester was recrystallized from methyl alcohol. 1,3,5-Tri(methoxycarbonyl)benzene was obtained with a yield of 96% (24 g). ¹H NMR (300 MHz, CDCl₃, ppm): δ 3.98 (s, 9H), 8.86 (s, 3H).

N¹,N³,N⁵-tris(2-aminoethyl)benzene-1,3,5-tricarboxamide (DT): In a three-neck round-bottomed flask (250 mL) equipped with a magnetic stirrer, a solution of compound 1 (8 g), ethylenediamine (6 g), methyl alcohol (100 mL) was refluxed for 12 h under nitrogen atmosphere. All the methyl alcohol and ethylenediamine were removed by vacuum distillation. DT was obtained with a yield of 86% (10 g). ¹H NMR (300 MHz, CD₃OD, ppm): δ 2.86 (t, 6H, *J*=7.6), 3.48 (t, 6H, *J*=6.7), 8.44 (s, 3H).

Polyhexamethylene Biguanide (PHMB): Equal molar ratios (1:1) of dicyandiamide and hexamethylene diamine were put into a 250 mL three-neck flask; the mixture was mechanically stirred while reaction temperature was kept at 150 °C for 2 h. Then the product was obtained after cooling. ¹H NMR (300 MHz, d-DMSO, ppm): δ 1.30 (s, 4H), 1.43 (s, 4H), 3.10 (s, 4H). FTIR (cm⁻¹): 3321 (brm), 2930 (s), 2855 (s), 2174 (m), 1660 (s), 1546 (s), 1435 (m), 1358 (m), 1280 (m), 1198 (s), 1151 (s), 720 (w), 610 (w).

Hyperbranched Polymer: In a three-neck round-bottomed flask (100 mL) equipped with a magnetic stirrer, a mixture of DT and PHMB was mechanically stirred while reaction tem-

perature was kept at 150 °C for 2 h under nitrogen atmosphere. A white solid product was received after cooling. ^1H NMR (300 MHz, D_2O , ppm): δ 1.30 (s, 24H), 1.53 (s, 24H), 2.81 (s, 6H), 3.11 (s, 24H), 3.43 (s, 6H), 8.24 (m, 3H). FTIR (cm^{-1}): 3376 (brn), 3168 (s), 2933 (s), 2859 (s), 1654 (vs), 1546 (s), 1475 (m), 1157 (s), 815 (w), 582 (brn).

Characterization of Hyperbranched Polymers. FTIR (KBr) spectra of the hyperbranched polymers were recorded by a Nicolet MX-IE Fourier transfer infrared spectrometer (Nicolet Japan). ^1H NMR spectra (AM 300 MHz nuclear magnetic resonance, Bruker USA) were used to characterize their molecular structures.

Antibacterial Properties. The qualitative and quantitative antimicrobial activities of antibacterials were demonstrated by several techniques. The MIC was determined by broth double dilution method.²⁷ In order to study the inhibition effect of hyperbranched DPB against bacterial growth, *E.coli* and *S. aureus* strain were grown on an agar plate, and their fresh colonies were transferred with the help of a sterilized loop into a shake flask, which was then incubated in an incubator shaker for 18 h at 37 °C at a shaking speed of 150 rpm under aerobic conditions. Culture media containing required nutrients was used for the cultivation.²⁸ 0.2 mL of the bacterial suspension was transferred into each test tube and then 1.8 mL of different concentrations of antibacterial were added in triplicate starting from 1000 to 0.1 $\mu\text{g}\cdot\text{mL}^{-1}$ (different tested concentrations were 1000, 100, 10, 1 and 0.1 $\mu\text{g}\cdot\text{mL}^{-1}$) into test-tubes just before inoculating with bacteria. 0.2 mL of the bacteria suspension was also added into 1.8 mL of double distilled water for the purpose to serve as a blank sample while measuring their OD at 700 nm. All these test tubes were placed in an incubator shaker for 24 h at 37 °C with a shaking speed of 150 rpm. There was a good linearity relationship between the bacterial biomass and the value of optical density at 700 nm. Therefore, the number of the bacteria of control groups and treated groups were monitored on the U-2010 spectrophotometer (Hitachi, Japan) by measuring the optical density at 700 nm. Then the results were expressed as the percent inhibition of bacterial growth. Inhibition percent was calculated by following eq. (1):

$$\text{Inhibition percent} = \frac{\text{OD}_{700 \text{ control}} - \text{OD}_{700 \text{ assay}}}{\text{OD}_{700 \text{ control}}} \times 100\% \quad (1)$$

Combined Antimicrobial Susceptibility Test. In order to investigate the effect of blending modification on the antibacterial activities, the combined antimicrobial susceptibility

tests between DT and DPB against *E.coli* were determined by paper strip test.²⁹ Two strips of filter paper that had been respectively dipped the antibacterial agent were placed vertically on the agar plate surface (see Figure 4(a)) that was inoculated with experimental strain (*E.coli*). Cultured at 37 °C for 24 h, the combined effect between antibacterial agents was determined according to the shape of the bacteriostatic zone.

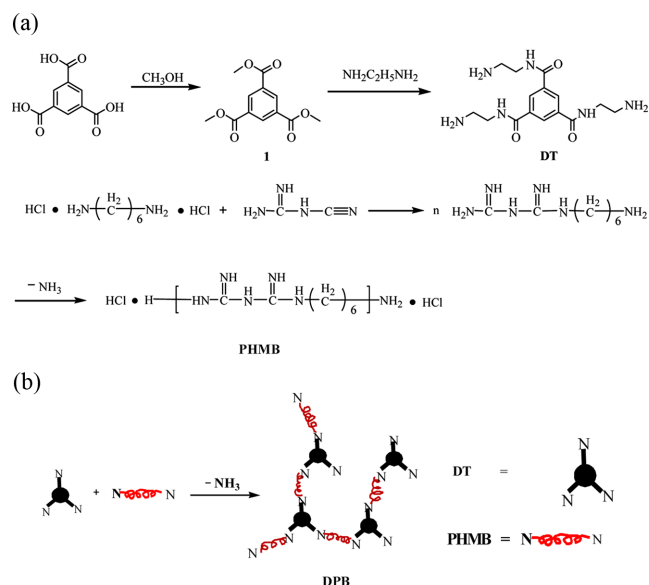
SEM Analysis. The preparation method of sample for SEM analysis: after centrifuging at 3000 rpm for 3 min, the *E.coli* cells were washed twice with PBS and redispersed with PBS solution. Hyperbranched polymer DPB1 with various concentrations were added into *E.coli* suspension and the mixtures were shaken for 30 min. Glutaraldehyde solution (2.5%) was added into the untreated *E.coli* and treated *E.coli* suspensions in order to fix the surface morphology of bacterial cells. Then the *E.coli* suspensions were centrifuged at 3000 rpm for 3 min, washed with PBS for three times and redispersed in PBS. The *E.coli* cells were dehydrated through a gradient series of ethanol (50, 70, 80, 90 and 100%, respectively) for 15 min and then air-dried in a vacuum desiccator. The images were observed with scanning electron microscope (SEM, Leitz-AMR-1000).

AFM Analysis. The untreated *E.coli* and treated *E.coli* samples were processed sequentially through the step of fixation, dehydration, dispersion. Then the *E.coli* cells were dropped onto a silicon wafer and air-dried in a vacuum desiccator. The morphological and profile images of *E.coli* were observed via atomic force microscopy (AFM, Veeco Nanoscope IIIa Multimode, USA).

Results and Discussion

Synthesis of Hyperbranched Biguanide Polymers. In this work, we designed and synthesized novel antibacterial functionalized DPBs by chemical doping of DT and PHMB with different reaction molar ratios. PHMB was firstly synthesized by condensation reaction from hexamethylene diamine and dicyandiamide, and then we integrated the antimicrobial property of hyperbranched polymers synthesized with PHMB and branched central core (DT). The reaction scheme was shown in Scheme 1. Hyperbranched products of DPB1, DPB2, DPB3 were obtained by $n_{\text{DT}}:n_{\text{PHMB}} = 1:1, 1:2$ and $1:3$, respectively. The molecular structure of PHMB and hyperbranched DPBs were characterized by FTIR, ^1H NMR spectra.

It was reported³⁰ that there were five characteristic peaks for



Scheme 1. Synthesis of hyperbranched polymer.

guanidine compounds as following: $\nu_{\text{N-H}}$ at about 3300 cm^{-1} , $\nu_{\text{C=N}}$ at $1689\text{--}1650\text{ cm}^{-1}$, $\delta_{\text{N-H}}$ at about 1640 cm^{-1} and $\nu_{\text{C-N}}$ at about 1300 cm^{-1} , $\delta_{\text{NH}^{2+}}$ at about $1620\text{--}1560\text{ cm}^{-1}$. The FTIR spectrum of the PHMB was shown in Figure 1. The FTIR spectrum revealed bands at 3321 (brm) , 1660 (s) , 1546 (s) , 1280 (m) cm^{-1} , corresponding to the biguanide group in PHMB. The 2855 and 2930 cm^{-1} peaks were assigned to the CH_2 -Symmetric stretching vibration (ss), CH_3 -ss mode, respectively.

The FTIR spectra of hyperbranched polymers (DPBs) were shown in Figure 2. The signals in the functional group region at 3376 , 1654 , 1546 , 1157 cm^{-1} were due to biguanide groups. Phenyl groups showed absorption for the C-H units at 3168 cm^{-1} and also lied in the range from 780 cm^{-1} (in the fingerprint region). The strong infrared absorption band of the C=O and the conjugated N-C(=N)-N stretching vibration were observed at 1654 cm^{-1} . With the increase in the content of PHMB, the N-H stretching vibration peak appeared at 3376 cm^{-1} became stronger slightly. The results confirmed that copolymerization took place as expected.

There were three characteristic peaks for ^1H NMR spectra (d-DMSO) of PHMB as following: 1.30 , 1.43 , 3.10 ppm . ^1H NMR spectra (D_2O) of DPB1 showed sharp peaks at 1.31 , 1.53 and 3.11 ppm , belonging to CH_2 units in PHMB. The peaks at 2.81 , 3.43 and 8.24 ppm were observed and assigned to methylene and phenyl groups in DT, respectively. According to the integral area of different hydrogen protons in Figure 3, the methylene protons' ratio between ethyl and hexyl group in DPB1 was $12:72$. Meanwhile, because DPB1 was obtained by

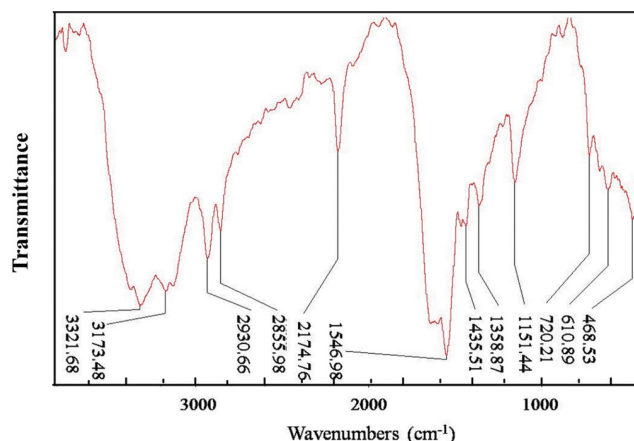


Figure 1. FTIR spectrum of PHMB.

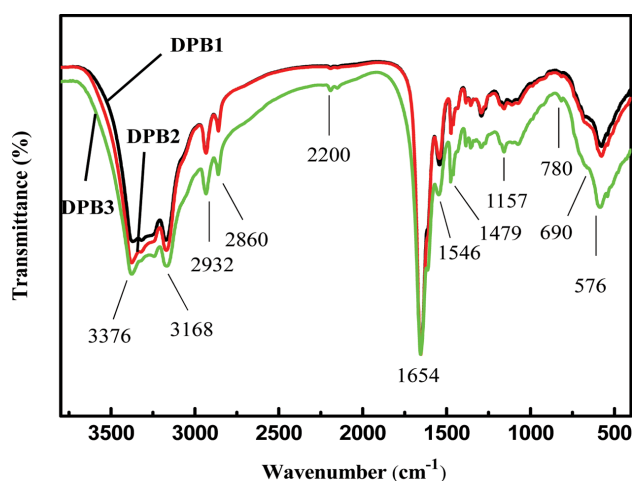


Figure 2. FTIR spectra of DPBs.

$n_{\text{DT}}:n_{\text{PHMB}} = 1:1$, we were able to calculate the molar mass of PHMB was about 1200 g/mol .

In terms of FTIR and ^1H NMR spectra, we could conclude that DPBs were synthesized successfully.

Antibacterial Activity. The novel synthesized hyperbranched compounds were evaluated for their antibacterial activities against Gram-negative (*E.coli*) firstly. The results of the inhibition zone, the minimum inhibitory concentration (MIC) were summarized in Table 1. The diameter of the inhibition zone of *E.coli* was studied using disk diffusion method.³¹ The average diameters of the inhibition zone of DPB1, DPB2 and DPB3 against *E.coli* were 6.8 , 6.0 and 5.9 cm , respectively. Determined by double dilution method, MIC of DPB1, DPB2 and DPB3 for *E.coli* were found to be 64 , 64 , 128 ppm , individually. These data suggested that DPB1 had a more excellent antibacterial activity than DPB2 and

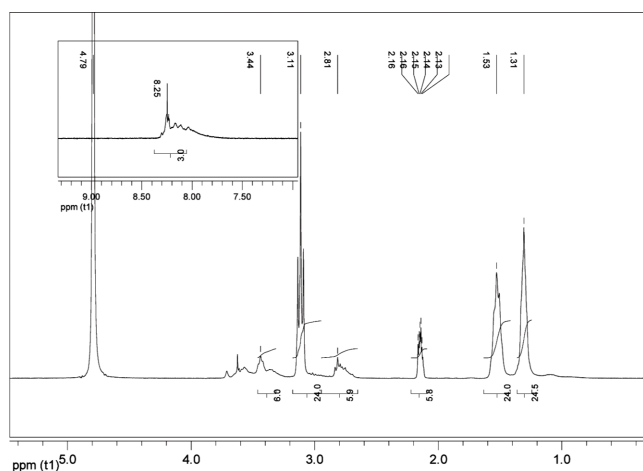


Figure 3. ^1H NMR spectra of DPB1 in D_2O .

DPB3. Meanwhile, MIC values of the hyperbranched DPBs were less than that of PHMB (256 ppm) and DT (128 ppm), which indicated the doping by chemical bond and structure modification could effectively improve the antibacterial activity of the antibacterials (see Table 1).

The bacterial growth inhibition rates of DPBs with various concentrations against *E. coli* (a) and *S. aureus* (b) were observed by UV-vis. The results were shown in Figure 4. As can be seen in Figure 4(a), treated with DPBs for 24 h, the *E. coli* inhibition rate enhanced with increasing concentrations. For example, the *E. coli* growth inhibition rates of DPB1 were 44.8%, 44.8%, 70.4%, 94.4% and 100%, when the concentrations were 10^{-1} , 10^0 , 10^1 , 10^2 and $10^3 \mu\text{g}\cdot\text{mL}^{-1}$, separately. Figure 4(a) showed that DPBs inhibited the growth of *E. coli* at a level as low as $10 \mu\text{g}\cdot\text{mL}^{-1}$ and effectively killed them at $100 \mu\text{g}\cdot\text{mL}^{-1}$. Similar results were reported for D3C1NC12.² The *E. coli* growth inhibition rate of DPB1 was higher than DPB2 and DPB3. That result may be due to the different spatial conformation of hyperbranched polymer. Because of the more compact nature of hyperbranched polymer, the more

Table 1. Antibacterial Activity of Antibacterials

| Antibacterials | MIC (ppm) | Diameter of inhibition zone (cm) |
|---|-----------|----------------------------------|
| PHMB | 256 | 4.0 |
| DT | 128 | 4.2 |
| DPB1 ($n_{\text{DT}}:n_{\text{PHMB}} = 1:1$) | 64 | 6.8 |
| DPB2 ($n_{\text{DT}}:n_{\text{PHMB}} = 1:2$) | 64 | 6.0 |
| DPB3 ($n_{\text{DT}}:n_{\text{PHMB}} = 1:3$) | 128 | 5.9 |
| Physical doping ($n_{\text{DT}}:n_{\text{PHMB}} = 1:1$) | 128 | 4.4 |

antibacterial cationic biguanide groups were encapsulated with increasing contents of PHMB in DPBs. The inhibition rate of DPBs against Gram-positive bacteria strain (*S. aureus*) was shown in Figure 4(b). The results also indicated that the inhibitory effect increased with an increasing concentrations of hyperbranched DPBs. For instance, at $1 \mu\text{g}\cdot\text{mL}^{-1}$, the hyperbranched DPBs inhibited the growth of *S. aureus*, but the bacteria could adjust to the environmental stress and survive. At a higher concentration ($10 \mu\text{g}\cdot\text{mL}^{-1}$), the growth inhibition rate increased very rapidly, almost 100%. With increasing the content of PHMB, the inhibition rate of DPBs declined. Compared with DPBs against *E. coli* strain, the growth inhibition rate of DPBs against *S. aureus* was significantly higher. The reason of this phenomenon was the difference in the structures of cell walls of Gram-positive and Gram-negative bacteria. In the Gram-positive bacteria, there were plenty of pores that allowed external molecules to come into the cell easily.³² However, there were two-layer membrane and cell wall in the Gram-negative bacteria. The outer membrane was a potential barrier

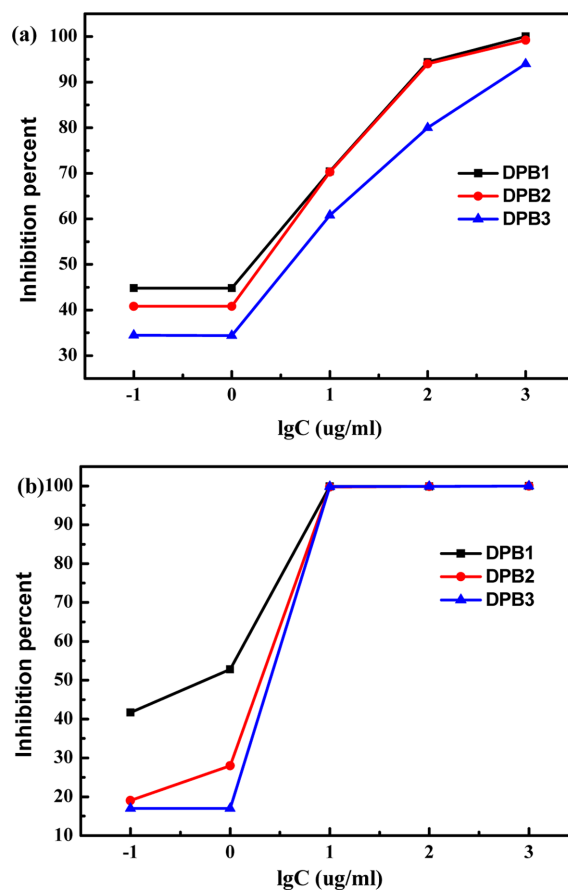


Figure 4. Growth inhibition rate of DPBs with various concentrations against *E. coli* (a); *S. aureus* (b).

against foreign molecules. Consequently, DPBs could more effectively kill Gram-positive bacteria than Gram-negative bacteria.

Combined Antimicrobial Susceptibility. As we know, the blending modification includes three types of physical blending, chemical blending, and physical/chemical blends, which can change the antibacterial activity of components. Taking two antimicrobial agents for an example, the combined effect of antibacterial agents utilizing the paper strip method used to define synergism, antagonism, and indifference (Figure 5(a)). In order to further verify the chemical blending could enhance the antibacterial activity, we observed combined antimicrobial susceptibilities of DT and PHMB against *E. coli* by paper strip test. From Figure 5(b), we noted no significant difference between DT and PHMB on inhibition area, which demonstrated the combined effect between DT and PHMB was indifferent. In other words, the physical doping of DT and PHMB could not improve their antibacterial activity. However, the diameter of inhibition zone of chemical blending product DPB1 (6.8 cm) against *E. coli* was bigger than that of DT (4.2 cm) and PHMB (4.0 cm) (see Figure 6), which evidenced the chemical modification of DPB1 with specific hyperbranched structure had more excellent antibacterial properties than physical blending.

Figure 7 displayed antibacterial effects of DT, PHMB, DPB1 with different concentrations against *E. coli* and *S. aureus* via

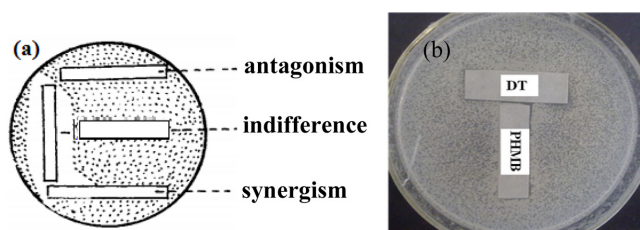


Figure 5. (a) Schematic diagram of the combined antimicrobial susceptibility test; (b) combined test of PHMB and DT against *E. coli*.

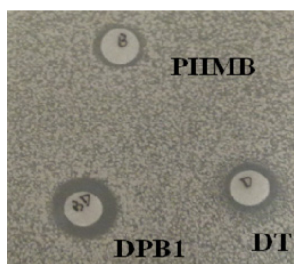


Figure 6. Inhibition zone of PHMB, DT and DPB1 against *E. coli*.

OD_{700nm} . The results suggested the inhibition effect of antibacterials against *E. coli* became stronger in the order of PHMB < DT < DPB1. For Gram-positive bacteria (*S. aureus*), bactericidal activity of antibacterials was consistent with Gram-negative bacteria. For example, at $10 \mu\text{g}\cdot\text{mL}^{-1}$, the OD_{700nm} value of hyperbranched DBP1 was 0.03, however, that of DT and PHMB were 0.28 and 0.20, respectively. At a higher concentration ($100 \mu\text{g}\cdot\text{mL}^{-1}$), the bacteria could be effectively killed by all antibacterial agents. In summary, all experimental results showed that DPBs had better comprehensive antibacterial properties than DT and PHMB for Gram-positive and Gram-negative bacteria, and the best one was DPB1.

Antimicrobial Mechanism of Hyperbranched DPB Revealed by SEM. SEM which could clearly provide the information of bacterial surface, was used to reveal the morphologic change of the microbial cells after treated with antibacterial agents. Figure 8 showed the morphological images of the fresh *E. coli* and the *E. coli* after the treatment. As can be

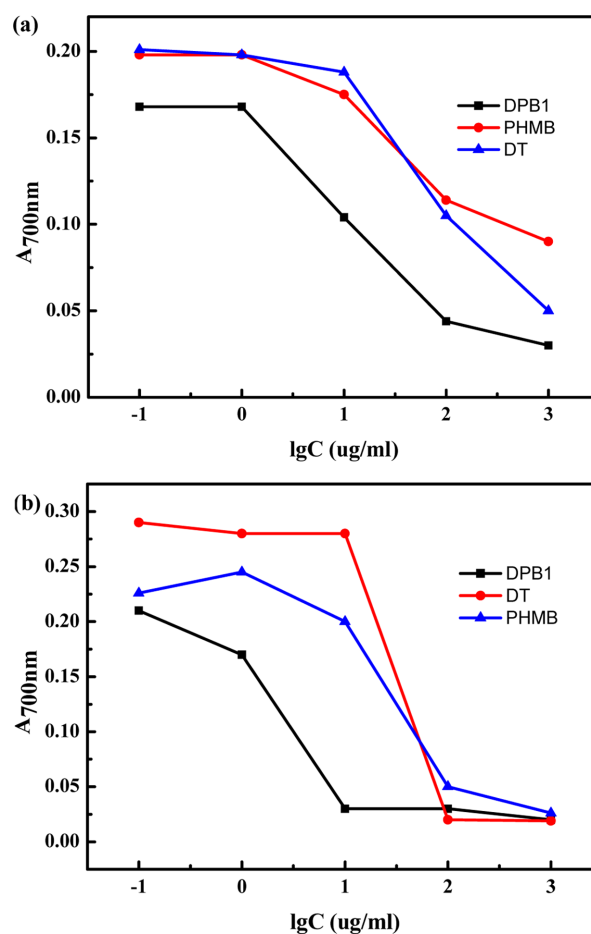


Figure 7. Antibacterial effects of DT, PHMB, DPB1 with different concentrations against *E. coli* (a); *S. aureus* (b).

seen in Figure 8(a), the rod-like *E.coli* showed a unique ellipsoid shape, and its surface membrane was integrated and smooth. In the presence of DPB1 at low concentration (50 ppm < MIC of DPB1), the rodlike morphology (*E.coli*) almost remained intact. However, there were many obvious grooves on the cell surface (see Figure 8(b)). The results indicated that the first effect of DPB1 in *E.coli* suspension was to interact with cytoplasmic membranes directly and to disturb the membranes, which also supported previous reports that the cell membrane was the principal target of cationic antibacterial agents,⁹ such as quaternary ammonium compound (QACs), guanidine and biguanide derivatives. At a higher concentration of DPB1 (200 ppm), most of *E.coli* strains were damaged severely and died, but there were still little bacterial cells have not been completely destroyed, in the form of collapsed rods (see Figure 8(c)). The SEM morphology showed that *E.coli* lost its discernable inner and outer membranes, which indicated most of the intracellular components had leaked via deformed membrane, such as K ions, DNA, and RNA.

AFM. The effect of the hyperbranched compound DPB1 on the *E.coli*'s cell surfaces was also examined by AFM. Figure 8 showed the AFM morphological and profile images of *E.coli* for (a) the control samples without DPB1, (b) samples in the presence of DPB1 at low concentration (50 ppm) and (c) samples in the presence of DPB1 at a high concentration (200 ppm). Morphological characterization of the *E.coli*'s cells generally showed typically rod-shaped cells of 250–300 nm height and 1.6–2.5 μm length. Often the cells also showed many pili or fimbria, typically extended on the glass surface.³³ The profile image in Figure 9(a) showed the *E.coli*'s cell with 1.5 μm length and 250 nm height, and the surface structure of the native *E.coli* was smooth. The morphological image in Figure 9(a) showed that there are many pili around the bacteria cell, which was also markedly observed by SEM image (Figure 8(a)). Figure 9(b) showed the influence on morphology of *E.coli* treated at low concentration of DPB1 for 30 min. The morphological image in Figure 9(b) displayed that *E.coli*'s surface had a few differences to the control bacteria, for instance,

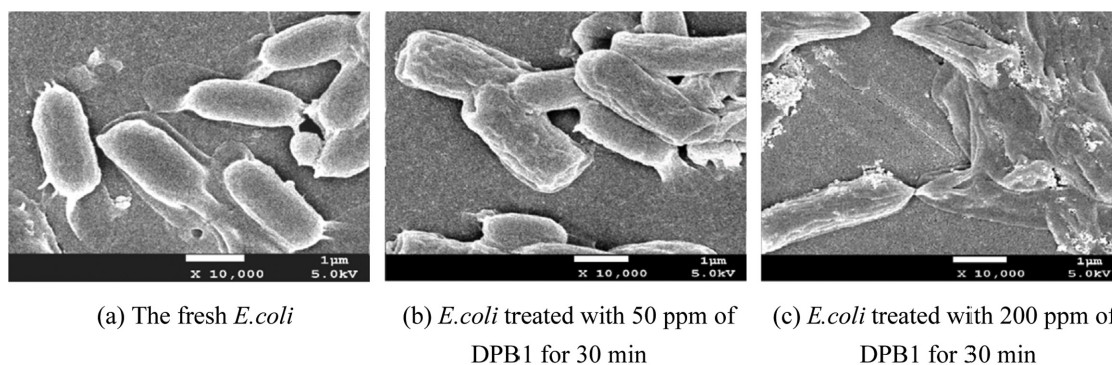


Figure 8. SEM images of *E. coli* treated with hyperbranched DPB1 with different concentrations.

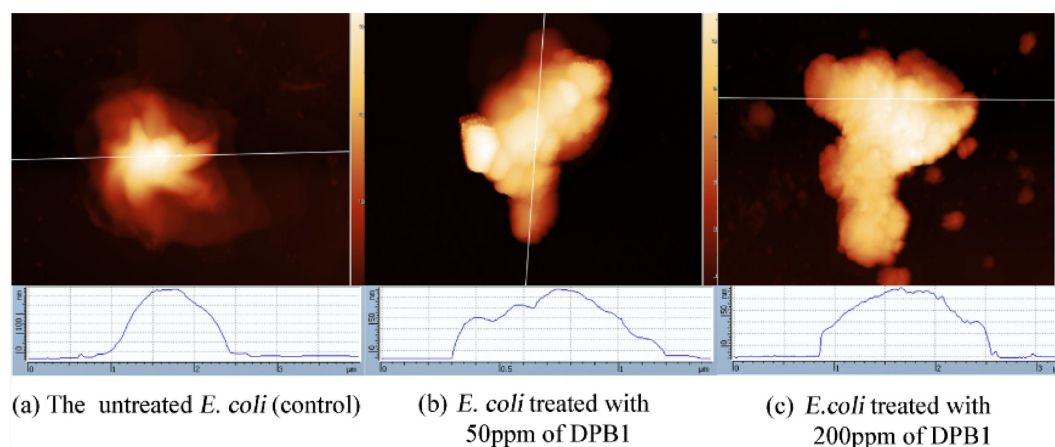


Figure 9. AFM images of untreated *E. coli* and *E. coli* treated with hyperbranched DPB1 with different concentrations.

the surface became rough. This phenomenon could also be evidently observed in profile image and SEM image (see Figure 8(b)). The height of bacterial cells reduced from 250 to 150 nm in the profile image, which indicated that few *E.coli*'s contents (potassium ions and phosphate) maybe have leaked from bacterial membrane, leading to the shrinkage of cells. It can be seen in Figure 9(c), the surface of *E.coli* was damaged severely, when they were treated with DPB1 at 200 ppm (a higher concentration) for 30 min. Due to the collapse of the *E.coli*'s membranes, most of the intracellular components were leaked, including DNA and RNA, leading to the death of *E.coli*. The height on the AFM profile graph reduced below 90 nm, which was also able to explain that the intracellular components were leaked.

AFM and SEM results could be interpreted on the basis of adsorption onto the bacterial cell surface, binding to the cytoplasmic membrane, disruption and disintegration of the cytoplasmic membrane, release of electrolytes such as potassium ions and phosphate, release of nucleic materials such as DNA and RNA, and the death of the cell, which were consistent with the typically mode of action of cationic antibacterials.^{9,32}

Conclusions

Since bacteria is negatively charged and the dendrimers or hyperbranched compounds have a high positive charge density, electrostatic interactions quickly bring them into contact with each other, which means that hyperbranched compounds have made available new opportunities for creating more potent antimicrobial agents for both industrial and biomedical applications. In this study, we demonstrated that it was feasible to synthesize the hyperbranched biguanide based antibacterial agents. Antibacterial DPBs that PHMB was integrated on DT branched central core was prepared via A2 + B3 reaction with different mole ratios using a one-pot synthesis. The antibacterial experimental results showed that DPBs, especially DPB1, had better comprehensive properties in the antibacterial area due to blending and structure modification. The antimicrobial mechanism of DPBs was revealed by visualizing the bacteria morphology with SEM and AFM images. The results were consistent with the typically mode of action of antibacterials, such as guanidine and QACs.

Acknowledgements: The authors gratefully acknowledge the financial support from the Opening Project of Zhejiang Key Laboratory of Clean Dyeing and Finishing Technology

(Grant No. 1402), Zhejiang Provincial Natural Science Foundation of China (Grant No. LQ15E080003), Zhejiang provincial Public Welfare Project (Grant No. 2017C31114), Shaoxing public welfare project (Grant No. 2015B70006), and the scientific research start-up funding of Shaoxing University (Grant No. 20145023, 20145033), School Research project Shaoxing University (Grant No. 2014LG1010), as well the helpness from Professor Zhengyong Qian and MS Ying Qu of Sichuan University.

References

1. J. Ding, B. Wang, and Z. Yue, *Angew. Chem. Int. Edit.*, **48**, 6664 (2009).
2. C. Chen, S. L. Cooper, and N. C. B. Tan, *Chem. Commun.*, **1**, 1585 (1999).
3. H. Wang, L. Zheng, C. Peng, M. Shen, X. Shi, and G. Zhang, *Biomaterials*, **34**, 470 (2013).
4. S. C. Han, J. W. Lee, and S. H. Jin, *Polym. Korea*, **38**, 386 (2014).
5. S. C. Han, S. H. Jin, and J. W. Lee, *Polym. Korea*, **36**, 295 (2012).
6. J. W. Lee, U. Y. Lee, and S. C. Han, *Polym. Korea*, **33**, 67 (2009).
7. M. Jikei and M. Kakimoto, *Prog. Polym. Sci.*, **26**, 1233 (2001).
8. P. Gilbert and L. Moore, *J. Appl. Microbiol.*, **99**, 703 (2005).
9. C. Z. Chen, N. C. Beck-Tan, and P. Dhurjati, *Biomacromolecules*, **1**, 473 (2000).
10. C. Z. Chen and S. L. Cooper, *Adv. Mater.*, **12**, 843 (2000).
11. A. Welk, C. Splieth, and G. Schmidt-Martens, *J. Clin. Periodontol.*, **32**, 499 (2005).
12. A. Kramer, V. Adrian, and C. Adam, *Hygiene und Medizin*, **18**, 9 (1993).
13. S. Gerli and F. Bavetta, *Eur. Rev. Med. Pharmacol. Sci.*, **16**, 1994 (2012).
14. E. Chadeau, C. Brunon, and P. Degraeve, *J. Food Safety*, **32**, 141 (2012).
15. Y. Gao, X. Yu, A. P. Pierlot, R. J. Denning, and R. A. Cranston, *J. Mater. Sci.*, **46**, 3020 (2011).
16. J. Kusnetsov, A. Tulkki, H. Ahonen, and P. Martikainen, *J. Appl. Microbiol.*, **82**, 763 (1997).
17. R. A. Rebong, R. M. Santaella, and B. E. Goldhagen, *Invest. Ophthalm. Vis. Sci.*, **52**, 7309 (2011).
18. L. Feng, F. Wu, J. Li, Y. Jiang, and X. Duan, *Postharvest Biol. Tec.*, **61**, 160 (2011).
19. C. R. Messick, S. L. Pendland, and M. Moshirfar, *J. Antimicrob. Chemoth.*, **44**, 297 (1999).
20. A. D. Lucas, E. A. Gordon, and M. E. Stratmeyer, *Talanta*, **80**, 1016 (2009).
21. M. Rosin, A. Welk, and O. Bernhardt, *J. Clin. Periodontol.*, **28**, 1121 (2001).
22. M. Rosin, A. Welk, T. Kocher, A. Majic-Todt, A. Kramer, and F. Pitten, *J. Clin. Periodontol.*, **29**, 392 (2002).
23. M. J. Allen, G. F. White, and A. P. Morby, *Microbiology*, **152**, 989 (2006).

24. Z. Jiang, B. Wang, H. Che, and B. Liu, *J. Macromol. Sci., A*, **49**, 952 (2012).
25. L. Qian, H. Xiao, G. Zhao, and B. He, *ACS Appl. Mater. Inter.*, **3**, 1895 (2011).
26. L. Qian, Y. Guan, B. He, and H. Xiao, *Polymer*, **49**, 2471 (2008).
27. J. M. Andrews, *Chemother.*, **48**, 5 (2001).
28. B. M. Guirard and E. E. Snell, "Biochemical factors in growth", in *Manual of Methods for General Bacteriology*, P. Gerhardt, R. G. E. Murray, R. N. Costilow, E. W. Nester, W. A. Wood, N. R. Krieg, and G. B. Phillips, Editors, American Society for Microbiology, Washington DC., p 79 (1981).
29. L. Heifets, *Am. Rev. Respir. Dis.*, **137**, 1217 (1988).
30. Y. Zhang, J. Jiang, and Y. Chen, *Polymer*, **40**, 6189 (1999).
31. I. Vandenbossche, M. Vaneechoutte, M. Vandevenne, T. De Baere, and G. Verschraegen, *J. Clin. Microbiol.*, **40**, 918 (2002).
32. A. Kanazawa, T. Ikeda, and T. Endo, *J. Polym. Sci.; Part A: Polym. Chem.*, **31**, 335 (1993).
33. P. Eaton, J. C. Fernandes, E. Pereira, M. E. Pintado, and F. X. Malcata, *Ultramicroscopy*, **108**, 1128 (2008).